International Journal of Sustainable Development and Planning
Vol. 15, No. 6, September, 2020, pp. 789-800
Journal homepage: http://iieta.org/journals/ijsdp

Groundwater Flow Dynamics and Distribution of Hydrochemical Facies Using GIS in Hodna Plain, M'Sila, Southeastern Algeria

Abdelouahab Amroune[1*], Redouane Mihoub[2], Guastaldi Enrico[3,4,5], Urena-Nieto Carlos[6]

[1] Faculty of Sciences, Department of Agronomiques Sciences, University of M'Sila, BP: 166, M'Sila 28000, Algeria
[2] Applied Renewable Energy Research Unit, URAER, Renewable Energy Development Center, CDER, 47133, Ghardaïa, Algeria
[3] CGT SpinOff S.r.l., Via E. Vezzosi, 15 - 52100 Arezzo, Italy
[4] GeoExplorer Impresa Sociale S.r.l., Via E. Vezzosi, 15 - 52100 Arezzo, Italy
[5] Center for GeoTechnologies, University of Siena, Via Vetri Vecchi, 34 - 52027 San Giovanni Valdarno, Italy
[6] University of Granada, Department of Geodynamics, Facultad de Ciencias, Campus de Fuentenueva s/n, 18071 Granada, Spain

Corresponding Author Email: abdelouahab.amroune@univ-msila.dz

https://doi.org/10.18280/ijsdp.150601

Received: 22 May 2020
Accepted: 28 July 2020

Keywords:
Algeria, Hodna aquifer, chemical facies, GIS, rock-water interaction, multivariate statistical

ABSTRACT

With the aid of the Geographic Information System (GIS), the present study aims to describe the relationship between groundwater flow systems and the distribution of chemical facies. The research also discusses the different geochemical processes which are responsible for the evolution of groundwater chemistry. Analytical studies of 25 groundwater samples indicate mean cation values such as Ca^{2+} (209.1 mg·l^{1-}), Mg^{2+} (116 mg·l^{1-}), Na^{+} (239 mg·l^{1-}) and K^{+} (2.8 mg·l^{1-}). The mean anion values are SO_4^{2-} (3.7 mg·l^{1-}), Cl^{-} (22.5 mg·l^{1-}), and NO_3^{-} (2.2 mg·l^{1-}). The GIS using topo to raster and multivariate statistical techniques were applied to the groundwater quality analyses obtained in order to define the major control factors that affect the plain hydrochemistry of Hodna. The statistical analysis reveals the presence of three groups, presenting an increased potential of salt content in the groundwater flow direction. Initially, in the aquifer boundaries and in the infiltration areas, the facies result as bicarbonate. In the southern part of the plain, groundwater becomes SO_4-Cl rich, because of the dissolution of salt formations and the presence of the Hodna salt water lake. The Cluster Analysis has described the effects of rock water activity and overexploitation of water intended for irrigation as being responsible for altering groundwater chemistry in the area. Rock-water interaction diagrams show chemical weathering caused by precipitation, along with dissolution of minerals forming soil. The scattered plots among ions revealed geochemical processes such as carbonate weathering, silicate weathering, cation exchange and reduction of sulphate.

1. INTRODUCTION

Groundwater is a vitally valuable resource worldwide. It has been estimated that about one third of the world's population uses freshwater to drink [1]. In the Algerian arid zone, the Hodna area is marked by a wide-open depression of 8500 km^2 surrounded by mountains, where the salt water lake "Chott El Hodna" ('salt water lake' in the local language) 1100 km^2 wide is located in the center. This morphology allowed the presence of a low endorheic hydrographic network that supplies surface water to the salt water lake, particularly during heavy random thunderstorms. The Chott is experiencing an excessive evaporation of both groundwater and surface water. Two aquifers, shallow and deeper, exist in this region, where irrigated agriculture has been established over the last 50 years [2]. Owing to excessive withdrawals, the water level in the shallow aquifer decreases sharply [3], inducing a significantly high salt concentration. On the other hand, the deeper aquifer with low salt concentration constitutes the main source of water in the plain [4].

Because of the broad extension of its hydrogeological watershed, its recharge would appear to be simple. The flow mechanism dynamics shows a local or regional impact on the natural spatial variability of groundwater chemistry [5]. This variation is caused by the absorption of ions in soils, sediments, and rocks, since the water flows within the pores and fractures of the unsaturated zone and the aquifer along mineral surfaces [6]. Nevertheless, due to over-exploitation by unregulated pumping, the piezometric level is gradually lowering [7]. This excessive drainage results in a gradual deterioration of the water quality in the irrigated region with the emergence of high salinity zones (EC > 3500 µS·cm^{1-}) and high nitrate contamination [8].

The groundwater flow mechanisms can be mapped and correlated to varying degrees with hydrochemical patterns [9]. [9] also pointed out that mapping groundwater flow systems will help to distinguish drinking water from non-drinking water. The large ions, that make up the bulk of the groundwater chemistry, operate as natural tracers, which are critical in delineating groundwater flow paths [10, 11].

Several statistical techniques have been applied to study, assess and characterize the chemical changes in groundwater such as Factor analysis (FA) and cluster analysis (CA) [4]. Utilized FA to study the geochemical evolution, mineralization and groundwater contamination. Additionally, the CA method was used to interpret the hydrochemical data based on factor scores, and to study the chemical evolution of water along groundwater flow [10]. The cluster analysis (CA), a statistical method for evaluating, determining and classifying chemical variations in groundwater, was utilized for hydro chemical data based on factor scores analyzing [12], and for the chemical evolution of water investigating along groundwater flow [13, 14].

The present study aims to describe the relationship between groundwater flow systems and chemical facies distribution, by using the Geographic Information System (GIS). The research would also describe the various geochemical processes that are responsible for the chemical production of groundwater chemistry.

2. MATERIALS AND METHODS

2.1 Study area

The area under investigation is located in the southeast of Algeria, between Mountains of Hodna (1863 m a.m.s.l.) in the north and Hodna Chott (450 m a.m.s.l.) in the south (Figure 1). The topography is an almost flat plain with a slope of no more than 2% and the highest altitude is 455 m a.m.s.l. The area is characterized by 215 mm, 19°C and 1700 mm of annual rainfall, temperature, and evapotranspiration. Temperatures rise as high as 50°C in summer [4]. This region is also characterized by rainfall with intense spatio-temporal variability [15]. The dryness condition has accentuated the water resource drawdown over the last decade, particularly because water regeneration has been very weak [4]. Dry atmosphere, atmospheric dust, and low precipitation rates affect the groundwater quality, usually causing a rise in salt content [4]. The region of research hosts over 150,000 people, spread throughout the plain. Agriculture, which remains the main occupation, especially for the production of vegetables and cereals like barley and corn, is being built according to the available water supplies, i.e. in the sandy area south of Chott El Hodna. According to Abdesselam et al. [16], the arable land area is 50,000 ha, 50% of which is irrigated. Conventional farming needs the use of fertilizers such as ammonium nitrate, urea, phosphorous and potassium, superphosphate, potassium chloride and, to a lesser degree, ammonium sulfate, sodium nitrate, calcium and potassium sulfate [4]. The lack of a treatment plant for wastewater causes the release of liquid waste in nature, flowing by easy absorption into the groundwater. The leaching of fertilizers utilized unnecessarily and without any monitoring harms the quality of the groundwater in the field of research.

2.2 Geological and hydrogeological setting

The geological map of the research area [17] shows the following main units: (1) Jurassic carbonate, (2) Cretaceous carbonate, (3) Mio-Pliocene clay and gypsum sand, and (4) Quaternary alluvial deposits (Figure 1). Jurassic and Cretaceous carbonate rocks, often with dense marl layers, are dolomitic limestone and sandstone about 550 m thick. The Mio-Plio-Quaternary Unit is characterized by heterogeneous continental detritus deposits, corresponding to red clay, sometimes lacustrine calcareous gypsum, conglomerates and alluvium. The thickness of this formation ranges from 300 to 500 m [2, 4].

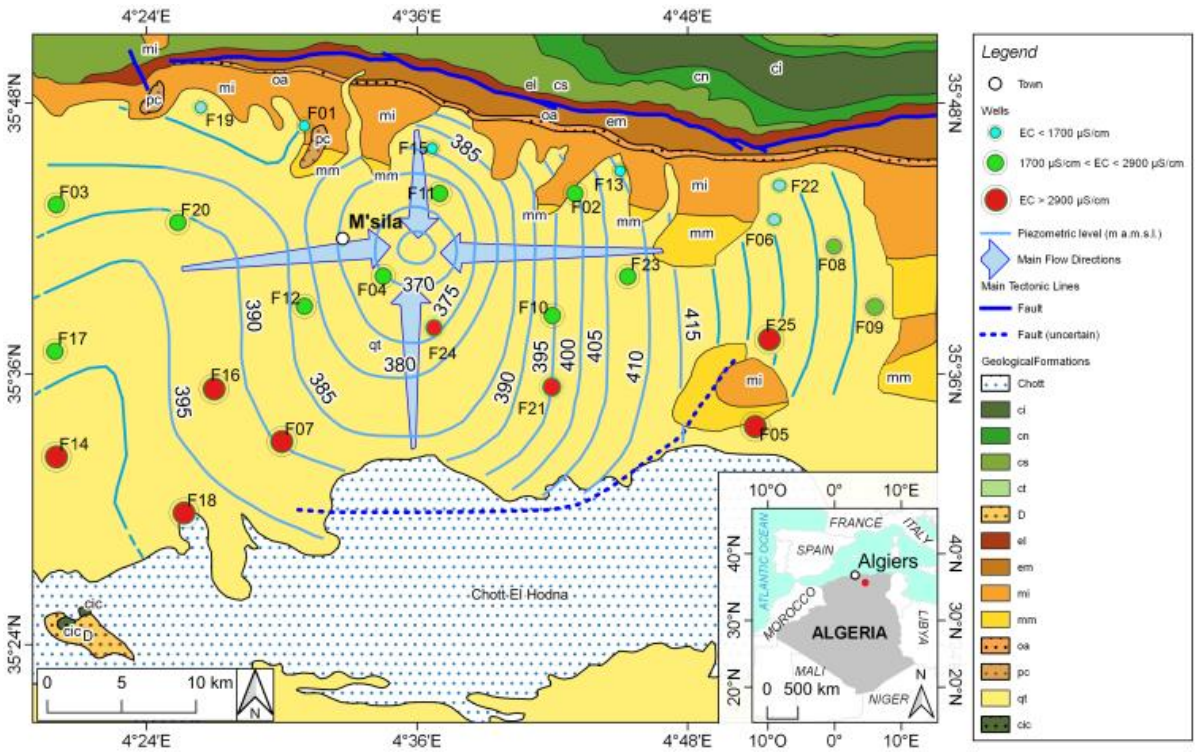

Figure 1. Situation of wells being sampled in the study area

Deep groundwater water table primarily exists below the surface at 10 m in the South and at 100 m in the north. Mio-Pliocene clays and marls, locally covered with gypsum, form the substratum of the shallow groundwater bearing complex. Pumping tests at different wells showed that the transmissivity varies from 10^{-5} $m^2 \cdot s^{-1}$ in the South to 10^{-2} $m^2 \cdot s^{-1}$ in the North [4]. The aquifer is recharged by meteoric water absorption in the basin and by surface water flowing from the North ridges surrounding the plain. This area is under heavy strain, both natural and anthropogenic, such as climate aridity, water resource overexploitation, and agricultural activities [8]. For several decades, major changes in land use and water resource use have been caused by successive agricultural policies in Algeria, the agricultural revolution, access to private land and the national agricultural development program [4, 16]. Piezometric examinations conducted during the dry season of 2012 showed a high piezometric level in the North, which dropped frequently towards the South, demonstrating the importance of hills for groundwater recharge. The main paths of groundwater flow converge to the middle of the plain (Figure 1). This groundwater settings indicates a recharge coming from the cretaceous calcareous in the North, while in the South by salt water lake, eventually a spill in the center is triggered by wells. This situation created an imbalance in the hydrogeological system, leading to a reversal flow, as seen in other parts of the world.

2.3 Sampling and analysis

In September 2012, 25 samples were taken to study the evolution of the physical-chemical parameters. Samples were obtained for stabilization of water temperature after a pumping period of 15 minutes, by means of two acid-washed polypropylene bottles. Each sample was immediately filtered in situ through 0.45 µm filters of acetate cellulose. Filtrate aliquots for cations analyses were transferred into 100 cm^3 polyethylene bottles and immediately acidified to pH<2 by the addition of Merck™ ultrapure nitric acid (5 ml 6 N HNO_3). Samples for study of anions were collected without acidification into 250 cm^3 polyethylene bottles. Both samples were placed in an ice chest at a temperature <4°C and eventually moved to the Constantine National Water Resources Agency Laboratory for study. Immediately after sampling, pH, Temperature (Tw), electrical conductivity (EC) parameters were measured in the field by utilizing a multi-parameter WTW (P3 MultiLine pH/LF-SET). The following chemical elements have been analyzed: calcium (Ca^{2+}), magnesium (Mg^{2+}), sodium (Na^{+}), potassium (K^{+}), chloride (Cl^{-}), bicarbonate (HCO_3^{-}), sulfate (SO_4^{2-}), and nitrate (NO_3^{-}). The samples were analyzed using American Public Health Association methods (APHA) [18]. By measuring the ion balance, the precision of the chemical analysis was checked; the errors were usually within 5% (Table 1).

The locations and altitudes of the boreholes were calculated using the Global Positioning System (GPS), to obtain the hydraulic head values the static water levels were subtracted from the altitudes. To define the different chemical facies characterizing each sample and the hydraulic head distribution, the results of the chemical analysis and hydraulic head values were implemented into the GW_Chart software [19]. A code was given to each of the chemical facies obtained from the GW_Chart program and then entered into the ESRI ArcGIS geo-data base to generate the water types spatial distribution map by interpolating data through Topo To Raster algorithm [20].

2.4 Multivariate statistical

Factor Analysis (FA) is often utilized in chemical data processing. Although FA is an exploratory and concise tool, it is also useful for classifying the key factors controlling groundwater chemistry [20]. The multivariate statistical method has been widely used to determine the environmental anomalies [21] and it has been successfully applied for hydrogeochemical processes studying [22] and for estimating the degree of mutually shared variability among individual pairs of water quality variables [23].

Joshi et al. [24] suggested using only variables above one's own interest. Under this criterion, only factors with their own values equal to or greater than 1 will be recognized as potential sources of data variation, attributing the highest priority to the factor with the highest individual vector amount. The justification for choosing the threshold 1 is that a factor must have a variance as high as that of a single standardized original variable in order to be acceptable [25]. Cluster Analysis (CA) is yet another method of data reduction, used in the grouping of entities with identical properties. The benefit of using CA's hierarchical approach is that it needs no prior knowledge of the cluster number [26]. CA contains a collection of multivariate approaches that are utilized for true data groups identifying [25, 26].

In the present study, CA was applied by using the Euclidian distance as a measure between the samples, and Ward's method as a linkage rule for the Hodna area classification of hydrogeochemical data.

2.5 GIS modeling

The ion concentrations form the base of geo-data to be interpolated by Topo To Raster for spatial distribution maps producting [20]. The ESRI ArcGIS Space Analyst incorporates a wide variety of cell-based GIS functions and among the three main types of GIS data, the raster data structure offers the most comfortable simulation framework and is used for spatial analysis [27]. The hydrochemical data considered for the modeling were TDS, Ca^{2+}, Mg^{2+}, Na^{+}, K^{+}, Cl^{-}, HCO_3^{-}, SO_4^{2-} and NO_3^{-}.

Topo To Raster tool was also utilized to produce the spatial distribution map of the various water facies. Topo to Raster is an interpolation method specifically designed for the creation of hydrologically correct digital elevation models (DEMs) [20, 28, 29]. It consists of a deterministic interpolation similar to the discretized spline, allowing to reproduce particular discontinuities in the modeled surface for that reason, Topo To Raster has been utilized for chemical data interpolating, since they are related to groundwater flow. The interpolation procedure has been designed to take advantage of the types of input data commonly available and the known characteristics of elevation surfaces. This method uses an iterative finite difference interpolation technique. Topo To Raster does not calculate the estimate errors in the unsampled space as the other deterministic interpolators, however, on the contrary of other methods such as the Inverse Distance Weighted function, it yields results that tend to represent the local variation of the known sampled values.

3. RESULTS AND DISCUSSION

3.1 Hydrogeochemical parameters of groundwater

Statistically the effects of groundwater quality data were presented in the form of minimum, average, mean, standard deviation and skewness (Table 1). pH of the water samples ranges from 7.01 to 8.23, with an average of 7.5, typical values of shallow aquifers in arid areas [24]. It is known that the processes of calcite and dolomite buffering are dominant for pH values ranging from 6.5 to 7.5 [30]. In addition, lithological formations include calcareous in an area where multiple redox reactions can occur, which causes carbonate dissolution. The groundwater is usually a little alkaline, but the consistency lies within the limiting value of the level of drinking water. The general increase of pH in a sedimentary terrain is related to plagioclase feldspar weathering in sediments. This phenomenon is aided by dissolved ambient carbon dioxide, resulting in sodium and calcium release, which slowly increases groundwater pH and alkalinity. 61% of pH measurements are contained in this range for the 25 groundwater samples studied.

Table 1. Statistical summary of hydrochemical parameters of groundwater. All values are in $mg \cdot l^{1-}$, except pH, EC in µS/cm

Wells	pH	EC	TDS	Ca^{2+}	Mg^{2+}	Na^{+}	K^{+}	Cl^{-}	SO_4^{2-}	HCO_3^{-}	NO_3^{-}
F01	7.71	1653	1340	269	99	50	5	401	277	544	26
F02	7.62	2150	1650	99	68	46	2	750	286	345	10
F03	7.25	2350	1860	222	124	191	1	228	849	233	22
F04	7.15	2140	1650	247	86	106	2	220	658	349	28
F05	7.01	3280	2230	452	228	554	2	309	1207	288	10
F06	7.45	1210	930	421	111	115	8	205	360	665	9
F07	7.36	3005	2330	100	81	554	1	516	920	294	4
F08	7.46	2300	1770	186	101	215	3	108	1032	254	6
F09	7.59	2653	2130	184	110	340	3	678	533	210	20
F10	7.62	2900	2560	177	139	400	3	835	743	260	1
F11	8.22	2200	1880	128	117	348	1	344	930	342	1
F12	7.12	2380	1940	200	168	325	6	476	1025	228	15
F13	7.85	1025	810	220	82	59	2	234	350	666	33
F14	7.48	3210	2620	149	146	420	5	845	733	251	1
F15	7.46	1554	1230	307	133	90	1	163	248	668	2
F16	8.23	3300	2470	119	138	318	1	344	918	346	5
F17	7.4	2827	2040	100	105	82	1	102	345	325	1
F18	7.42	3088	2670	99	107	507	2	518	925	288	4
F19	7.10	1622	1145	233	75	65	3	196	265	661	29
F20	7.54	1745	1233	245	86	74	5	369	956	366	2
F21	8.01	3105	2815	102	156	276	2	651	521	204	11
F21	7.23	1123	876	356	91	81	2	168	253	736	3
F23	7.36	1087	821	389	88	56	1	124	1120	271	1
F24	7.24	3256	2781	125	123	391	4	539	1005	241	2
F25	7.74	3048	2801	98	138	312	3	625	501	219	22
Min	7.01	1025	810	98	68	46	1	102	248	204	1
Mean	7.50	2328.4	1863.3	209.1	116.0	239.0	2.8	397.9	678.4	370.2	10.7
Max	8.23	3300	2815	452	228	554	8	845	1207	736	33
SD	0.32	770.6	673.7	106.9	35.4	170.6	1.8	232.6	318.2	172.9	10.5
Skew	0.8	-0.3	-0.1	0.9	1.3	0.4	1,3	0.5	0.0	1.1	0.9
AHG	6.5-9	2800	1500	200	/	200	12	500	400	/	50

Min: minimum value; Mean: average value; Max: maximum value; SD: standard deviation; Skew: skewness; AHG: Algerian health guidelines

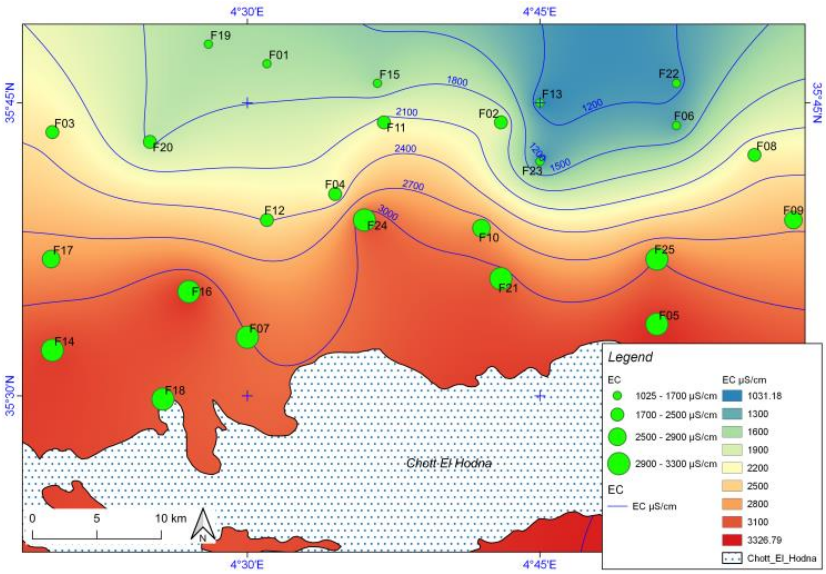

Figure 2. Spatial distribution of EC concentrations in the study area

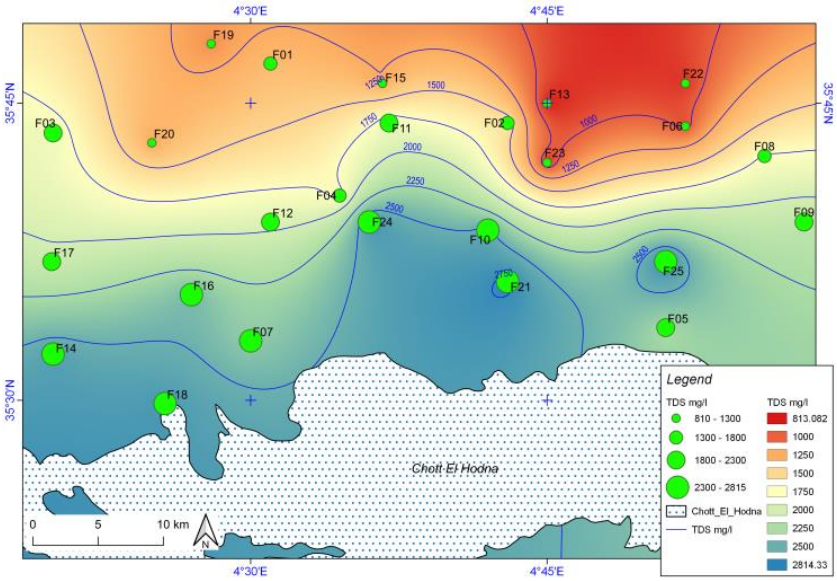

Figure 3. Spatial distribution of TDS concentrations

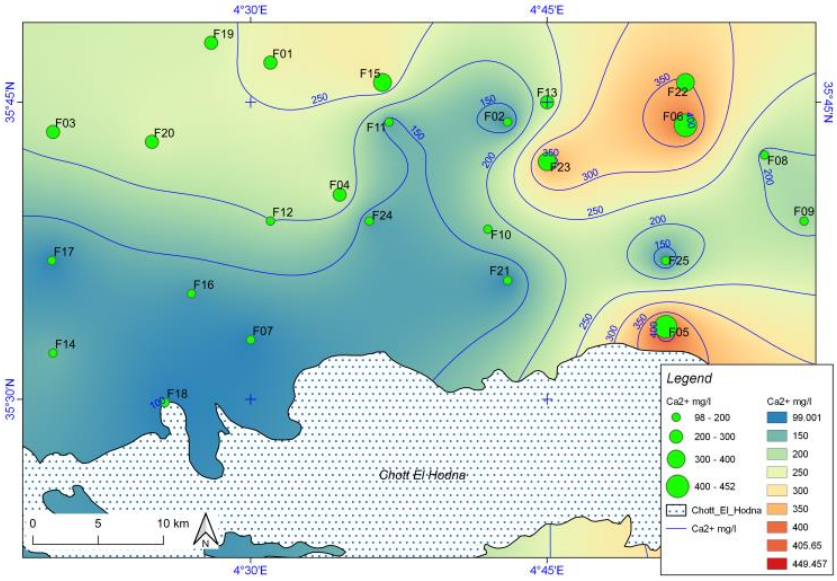

Figure 4. Spatial distribution of Ca^{2+} concentrations in the study area

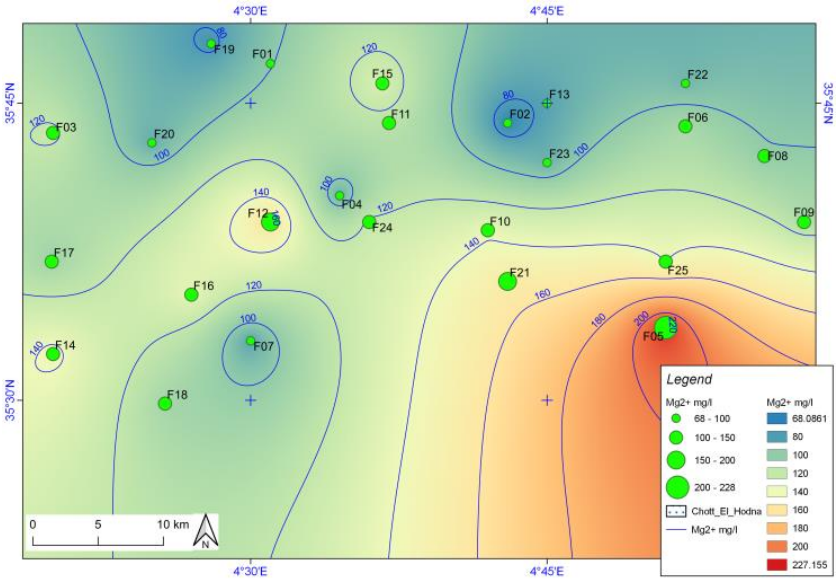

Figure 5. Spatial distribution of Mg^{2+} concentrations in the study area

EC and TDS range from 1025 µS·cm^{-1} to 3300 µS·cm^{-1} and 810 mg·l^{-1} to 2815 mg·l^{-1}, with mean values of 2328 µS·cm^{-1} and 1863 mg·l^{-1}, respectively (Table 1, Figures 2 and 3). Ca^{2+} ranges also from 98 mg·l^{-1} to 452 mg·l^{-1}, with a mean value of 209.1 ± 106.9 mg·l^{-1} (Table 1, Figure 4). Mg^{2+} varies from 68 mg·l^{-1} to 228 mg·l^{-1}, with the mean value of 116 ± 35.4 mg·l^{-1} (Table 1, Figure 5). Na^{+} varies from a minimum of 46 mg·l^{-1} to a maximum of 554 mg·l^{-1}, with a mean value of 239 ± 170.6 mg·l^{-1} (Table 1, Figure 6). K^{+} ranges from 1 mg·l^{-1} to 8 mg·l^{-1}, with a mean value of 2.8 ± 1.8 mg·l^{-1} (Table 1, Figure 7). Alkalinity varies from 204 mg·l^{-1} to 736 mg·l^{-1}, with a mean value of 370.2 ± 172.9 mg·l^{-1} (Table 1, Figure 8). SO_4^{2-} ranges from 248 mg·l^{-1} to 1207 mg·l^{-1}, with a mean value of 678.4 ± 318.2 mg·l^{-1} (Table 1, Figure 9). Cl^{-} varies from 102 mg·l^{-1} to 845 mg·l$^{-1,}$ with a mean value of 397.9 ± 232.6 mg·l^{-1}. NO_3^{-} varies from 1 to 33 mg·l^{-1}, with the mean value of 10.7 ± 10.2 mg·l^{-1}. Higher mean values of Na^{+}, Cl^{-}, and SO_4^{2-} indicate a likely contamination by high salinity waters of the lake and a dissolution of evaporate minerals.

The abundance of the major anions is SO_4^{2-}>Cl^{-}>HCO_3^{-}, 68% of samples exceeded the maximum acceptable concentration of SO_4^{2-} for drinking water (400 mg·l^{-1}), and 36% of samples overcame the maximum acceptable concentration of Cl^{-} for drinking water (500 mg·l^{-1}). The abundance of the major cations is Na^{+}>Ca^{2+}>Mg^{2+}>K^{+} and 52% of samples exceeded the maximum acceptable concentration of Na^{+} for drinking water (200 mg·l^{-1}), whilst 44% of samples showed values of Ca^{2+} higher than the maximum acceptable concentration for drinking water (200 mg·l^{-1}) [31].

3.2 Groundwater flow process and chemical facies distribution

Salinity, represented by the EC (Figure 1), increases from the center of the plain to the salt water lake. This is the result of the inversion of the flow from the salt water lake towards the plain, due to the drawdown induced by pumping. For water samples along the northern piedmont, low values (EC<1700 µS·cm^{1-}) were reported and constitute 28% of cases (Group 1, G1). As shown by the piezometric map they correspond to the recharge region.

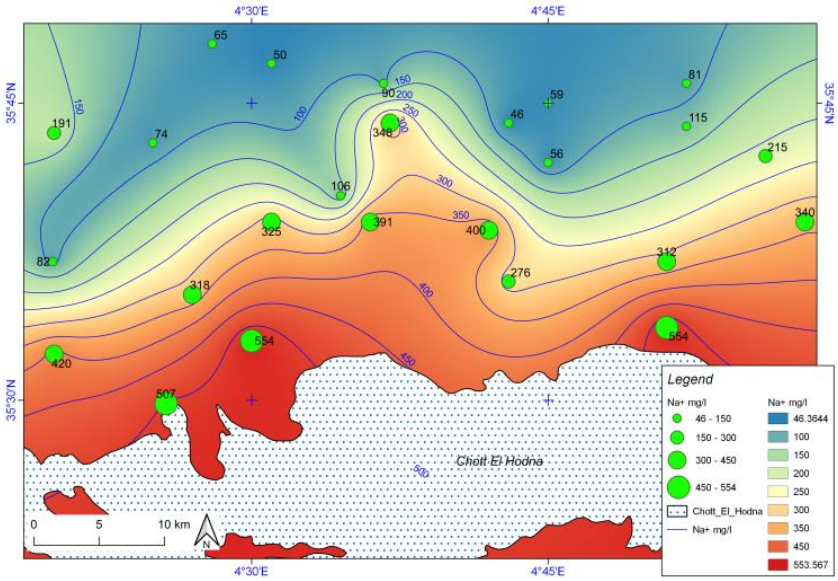

Figure 6. Spatial distribution of Na^{+} concentrations in the study area

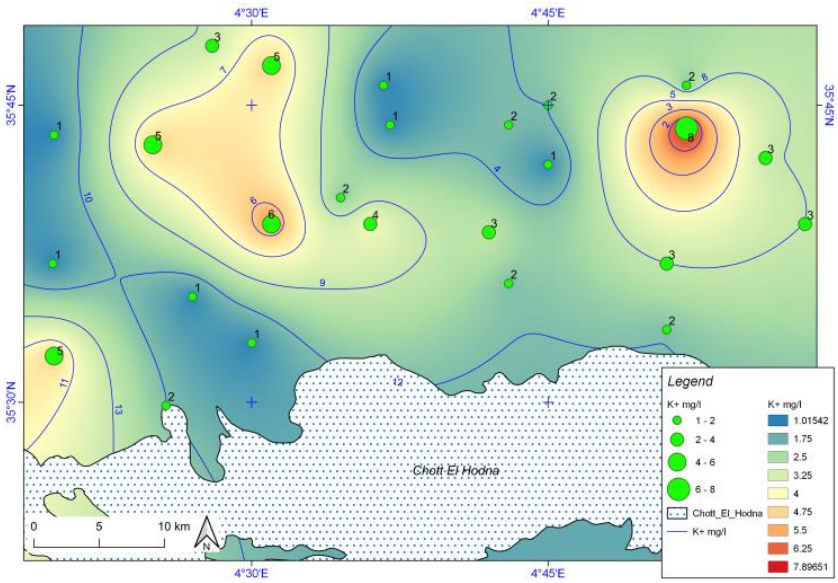

Figure 7. Spatial distribution of K^{+} concentrations in the study area

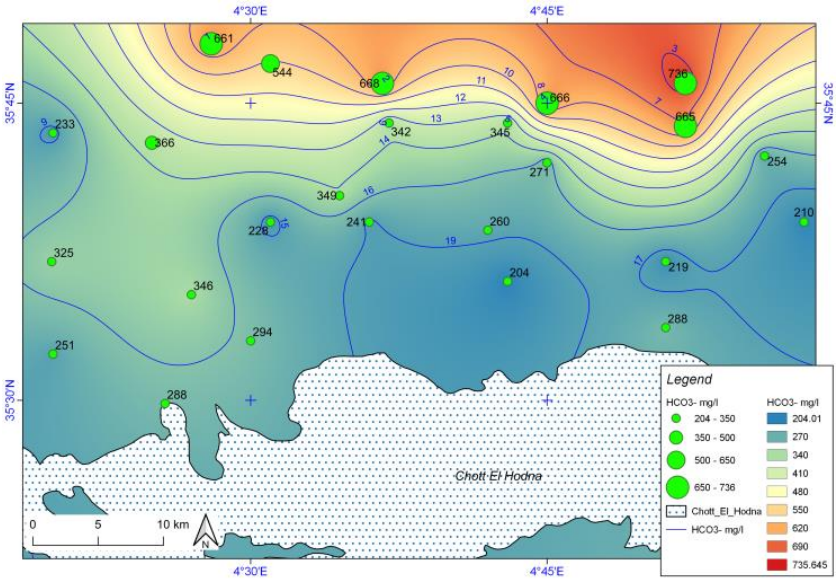

Figure 8. Spatial distribution of HCO_3- concentrations in the study area

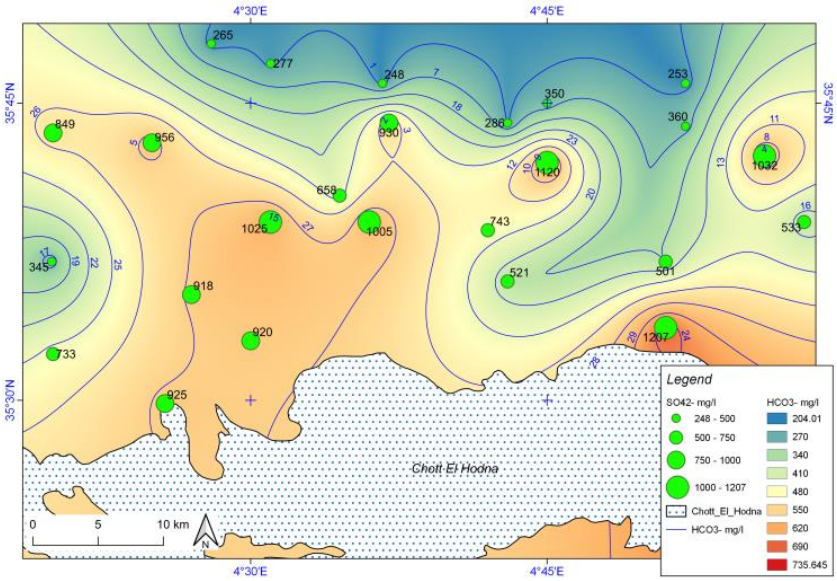

Figure 9. Spatial distribution of SO_4^{2-} concentrations in the study area

The second group of samples (G2) shows salinity ranging from 1700 to 2900 µS·cm^{1-} and makes up 40% of cases. It characterizes those samples that are obtained from the center plain. The third group (G3) has a higher salinity values than this cap and represents 32% of instances, located close to the salt water lake.

The key causes are the introduction of residual solids into the aquifer, and the water flow through low soluble mineral sediments.

Samples of groundwater were plotted in a diagram (Cl^-vs Ca^{2+}+Mg^{2+}) [32] to display the different forms of water in the study region (Figure 10). This diagram shows that the chemical character in general falls within the following types of water:

- Fresh groundwater with low salinity concentrations, located in the northern part of the study area;
- Saline water with high salinity concentrations, located in the southern part.

Situated in the nearby Hodna Lake, these salt water samples reflect the effect of salty water intrusion and related processes (halite and gypsum dissolution) and anthropogenic contamination at the well head.

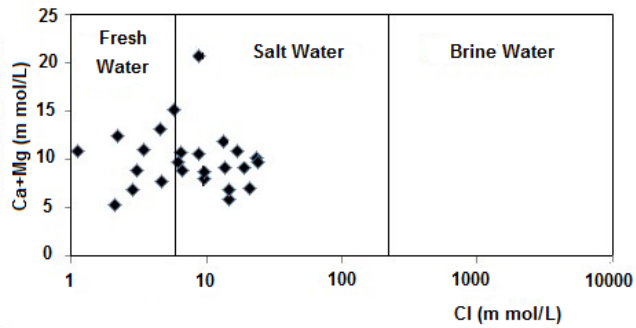

Figure 10. Cl versus Ca and Mg in mmol/l for groundwater samples

The different water samples have been classified according to their chemical composition using the Piper diagram (Figure

11). The analysis showed that the water grade calcium-bicarbonate (Ca^{2+}-HCO_3^-) characterized 24% of the samples, primarily located in the north of the region of study. The presence of fractured and karst carbonate formations on the northern boundary indicates a rainwater infiltration where they develop a calcite facies, which explains the existence of low salinity water (EC<1700 µS·cm^{1-}) on the northern part. SO_4^{2-}-Cl^--Na^+ water type characterizes 32% of all the samples collected, and this condition is mainly detected along the salt water lake, in the southern part of the study area. This explains the presence of high salinity (EC>2900 µS·cm^{1-}) water in that portion of the study area. These facies are linked to sandy formations, such as marl and clays around the salt lake. The remaining water samples (40%) are intermediate types of water between those mentioned above, and are sulfate-dominant types (SO_4^{2-}-HCO_3^--Ca^{2+}, SO_4^{2-}-Ca^{2+}-Mg^{2+}, SO_4^{2-}-Ca^{2+}, SO_4^{2-}-Na^+-Ca^{2+}, and SO_4^{2-}-Cl^-). In this category the electrical conductivity ranges from 1700 to 2900 µS·cm^{1-}, pecurial of the mixed water. Therefore, the water type Ca^{2+} - HCO_3^- reflects the replenishment and regeneration from the recent meteoric water, while the water type SO_4^{2-}-Cl^--Na^+ suggests leaching of the salt deposit aquifer matrix (Figure 12).

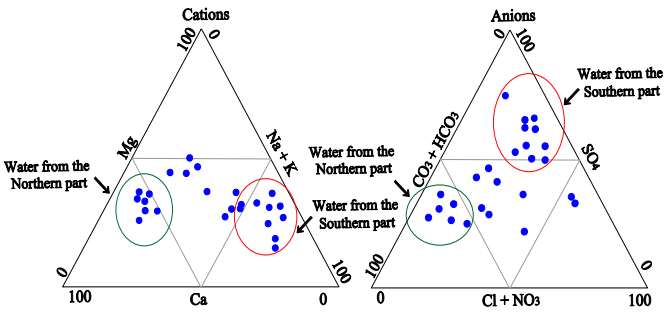

Figure 11. Diagram Piper applied to water samples of Hodna aquifer

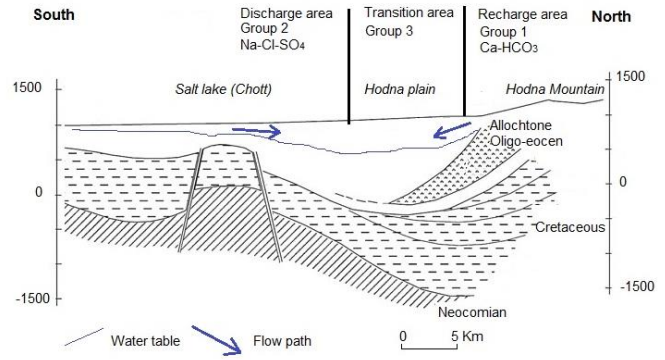

Figure 12. Schematic section along the groundwater flow path

3.3 Statistical analysis

3.3.1 Factor analysis

The FA was conducted on 25 individuals and 9 variables (EC, Ca^{2+}, Mg^{2+}, Na^+, K^+, Cl^-, SO_4^{2-}, HCO_3^-, and NO_3^-). Table 2 displays the individual values of the variables derived and the proportion of the overall survey variation described by the variables. The study yielded 10 variables, but only three variables have been preserved, accounting for 81% of the overall variance. The parameter's weights for the three factors of the dataset are given in Table 2. EC, Na^+, Cl^- and SO_4^{2-} marked factor 1, which explained 52% of the variance, it has a strong to moderate positive loading in EC, Na^+, Cl^- and SO_4^{2-}, which are 0.77, 0.78, 0.63, and 0.70 respectively. High positive charges indicated a strong linear correlation between the parameters and the factor. Factor 1 may therefore be regarded as a cause for salinization. Simultaneous drought and overexploitation caused the groundwater level to deteriorate. Such variables suggest this is the aquifer's effect on various forms of soil. Groundwater aquifer, containing evaporite host rocks, can achieve large Cl^- and SO_4^{2-} concentrations.

Factor 2 explains 22% of the total variance, it has a moderate negative loading in Mg^{2+}, Ca^{2+} and HCO_3^-, which are –0.68, –0.56 and –0.55 respectively. These variables indicate the existence of an influence of the aquifer by the types of carbonate rock.

Table 2. Variance explained and component matrixes

	Factor 1	Factor 2	Factor 3
EC	0.77	0.43	0.39
Mg	0.32	-0.68	0.49
Ca	0.06	-0.56	0.09
Na	0.78	0.43	0.43
K	-0.32	-0.33	-0.48
Cl	0.63	-0.38	0.04
SO_4	0.70	-0.62	-0.19
HCO_3	-0.05	-0.55	0.07
NO_3	-0.08	0.18	-0.68
Eigenvalue	2.98	2.02	0.59
Variance (%)	53	22	7
Cumulative (%)	53	75	82

Factor 3 explains 7% of the total variance of the dataset; it shows a significant characteristic with K, Cl^-, and NO_3^-. It has strong negative loadings on NO_3^- (–0.68) and weak loading on K^+ (–0.48). Factor 3 is concerned mainly with host evaporite rocks and chemical fertilizers. Huge quantities of fertilizers, such as urea and industrial compounds, have long been added. NH, the basic ingredient of fertilizers, is readily oxidized to NO_3^- under oxidation conditions by the nitrification cycle [33].

3.3.2 Cluster analysis

Clusters can be defined using two separate approaches, namely R or Q-modes [34]. R-mode is typically applied to water quality variables for their interactions highlighting, while Q-mode shows the relationships between the tested samples. In this study eight calculated hydrochemical variables (Ca^{2+}, Mg^{2+}, Na^+, K^+, Cl^-, SO_4^{2-}, HCO_3^-, and NO_3^-) were utilized.

The Ca^{2+}, Mg^{2+} and HCO_3^- concentrations may be regarded as the variables representing the phase of dissolution of carbonates that occurs in the boundary areas during the aquifer recharge. On the other hand, the variables Cl^- and SO_4^{2-} may be defined as being indicative of other alternate salinization of the Hodna aquifer groundwater, as the variables representing the phase of the Hodna Lake salt water intrusion. Thus, Na^+, K^+ and NO_3^- coming from the solute return flow from irrigation production may also be viewed as an applied method for salinization. Such factors can be contained in the phases of natural mineralization and anthropogeny. The non-homogeneous existence of the aquifer culminated in numerous hydrogeochemical facies for groundwater such as Ca^{2+}-HCO_3^- in the northern fringe and SO_4^{2-}-Cl^--Na^+ in the southern plain.

The G1 has a low salinity (EC<1700 µS·cm^{1-}), while G2 shows high salinity (EC>2900 µS·cm^{1-}), and G3 both intermediate and average salinity (1700<EC<2900µS/cm). These

groups of the samples are located in different areas. The G1 is located in the north, near the recharge zone, the G2 in the south, near the salt water lake and the G3, in the center of the plain (Figure 13). The G1 consists of wells 1, 2, 6, 13, 15, 19 and 22, it is defined by both Ca^{2+} and HCO_3^-. It is situated at the geological outcrops to the North. G2 is located primarily in the South of the research region near the salt water lake. This category includes the 5, 7, 10, 14, 16, 17, 18, 21, 24 and 25 wells. This is affected by the salivary deposits of the Triassic as well as by the salt water lake returns flow and is defined by SO_4^{2-}-Cl^-. G3 is a transitional time between the two severe classes, originating from the wells 3, 4, 8, 9, 11, 12, 20 and 23 and distinguished by Na^+, K^+ and NO_3^- from the agricultural activity.

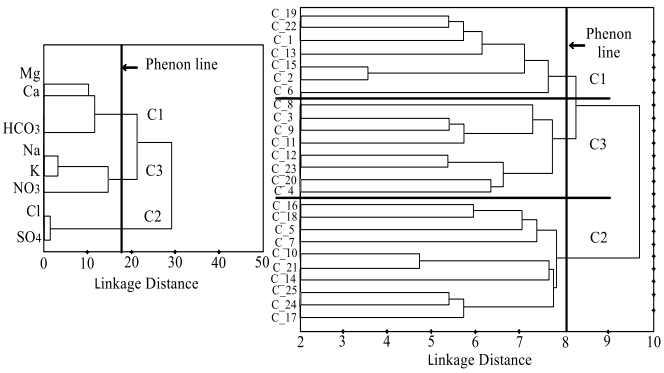

Figure 13. Dendrogram of cluster analysis of variables and the hydrochemical samples

3.3 Water–rock interaction process

The ions leached out and dissolved in reservoirs through weathering and water absorption in rocks and soils [35]. The geological forms, water-rock contact, and ion relative mobility are prime factors that affect groundwater geochemistry [36]. The use of distributed plots for TDS vs Na / (Na+Ca) and TDS vs. Cl / ($Cl+HCO_3$) [37] can be used to evaluate mechanisms of rock-water interaction processes. The Gibbs ratios are calculated by the formulae 1 and 2 given below:

$$\text{Gibbs Ratio I (for Anion)} = Cl^-/(Cl^- + HCO_3^-) \quad (1)$$

$$\text{Gibbs Ratio II (for Cation)} = Na+/(Na^+ + Ca^{2+}) \quad (2)$$

where, all ions concentrations are expressed in mmol/l.

The different water samples have been classified according to their chemical composition using Gibbs diagram (Figure 14). The predominant samples (64%) fall into mixing and few (20%) samples into fresh water. Gibbs ratio I values in the present study vary from 0.28 to 0.85, with an average value of 0.61, while Gibbs ratio II values vary from 0.13 to 0.95, with an average value of 0.72. The first form of water is constantly modified due to both the effects of the water-rock relationship of the aquifer stone, which is made mostly of evaporite facies, and the impacts of human activities, and finally the return flow of irrigation. The effect is demonstrated by a large rise in concentrations of sodium, sulfate, and chloride in groundwater. The second form of water at northern boundary is affected by carbonate rock.

Controls of groundwater's hydrochemical evolution primarily rely on recharging water chemistry, water aquifer matrix activity, or both, as well as groundwater residence period within the aquifer. Two basic mechanisms lead to the deposition of solutes in groundwater: dissolution by evaporation and dissolution of carbonate [38]. Evolving water's chemistry relies not only on the matrix's bulk chemistry, but also on the weathering rate [39]. Therefore, only comparatively low concentrations of carbonates and evaporates may have a substantial effect on water chemistry [26]. We utilized the ion connection diagrams of the major elements produced in molar concentrations for these hydrogeochemical processes clarifying. Variation of the evaporate components influenced the first diagram. The Na^+ vs Cl^- relation reveals that the majority of water samples contribute to a regression straight line with a 0.71 slope, significantly different from the slope 1 of the halite dissolution (Figure 15a). Therefore, Na+ and Cl^- are largely derived from the dissolution of halite [40], since the geological environment is very rich in evaporite minerals. The second diagram Ca^{2+} + Mg^{2+} vs SO_4^{2-} + HCO_3^- can highlight the origin of Ca^{2+}, Mg^{2+} and SO_4^{2-}. Hence, it is evident that the chemistry of the water in the area is usually determined by the dissolution of calcite, dolomite and gypsum and by the interaction of ions, or the salinity is induced by the impact of the Hodna Lake (Figure 15b). This is also verified in the third Ca^{2+} vs SO_4^{2-} diagram (Figure 15c). The infiltration of the rain water through the carbonate formations in the northern part of study area allows the dissolution of limestones and dolomites of Cretaceous and Jurassic. During the groundwater flowing, the water allows the dissolution of gypsum and/or anhydrite in Mio-Plio-Quaternary age. The last diagram Ca^{2+}+Mg^{2+}+HCO_3^- /Na^++K^++Cl^-+SO_4^{2-} vs TDS can demonstrate the global origin of salinity (Figure 15d). In fact, in this diagram two groups can be individualized by their salinity: samples with low salinity (TDS<1700 mg·l^{1-}) dominated by carbonates coming from the northern part, and those with high salinity (TDS>1700 mg·l^{1-}) dominated by salty minerals from the southern part.

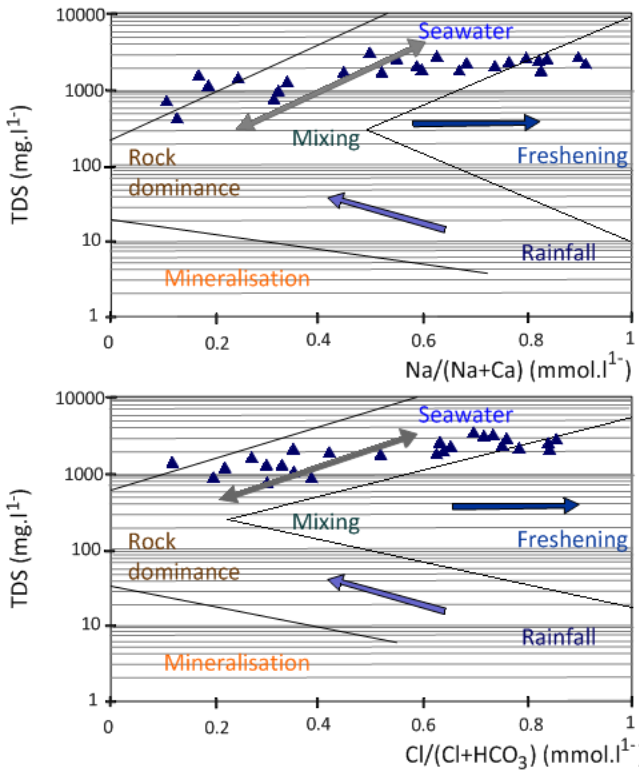

Figure 14. Gibbs diagrams for water samples of the Hodna aquifer

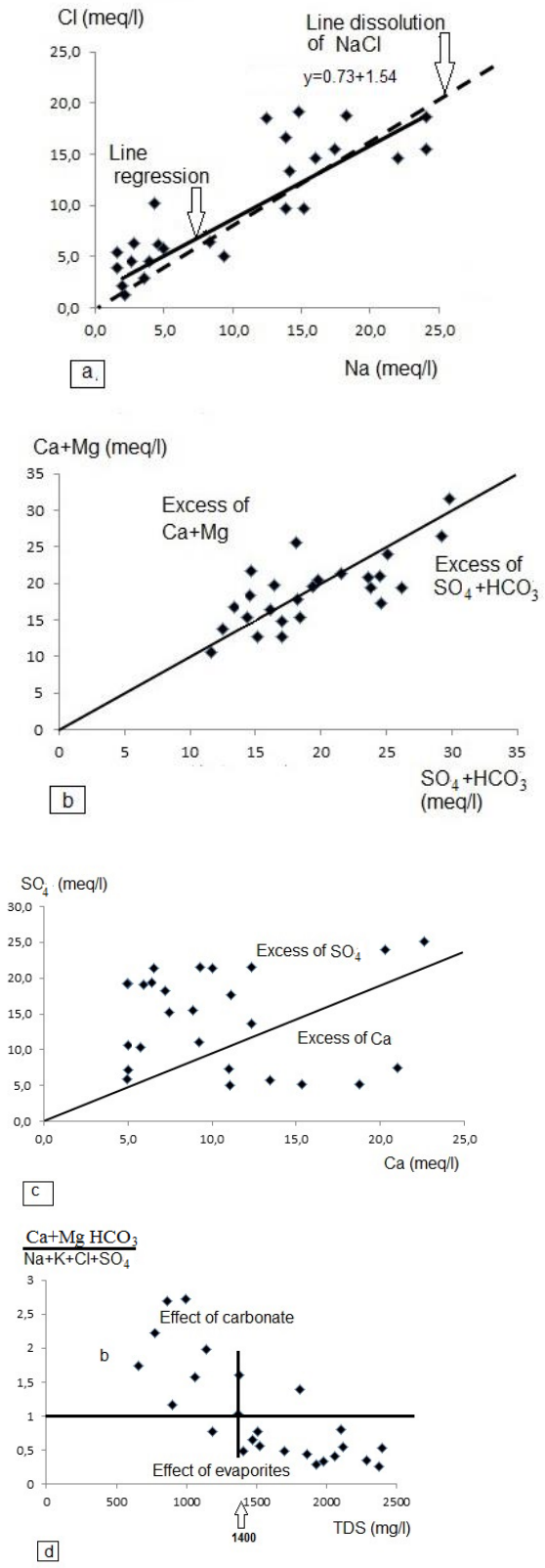

Figure 15. Plot of (a) Na^+ *vs* Cl^- (b) $Ca^{2+}+Mg^{2+}$ *vs* $SO_4^{2-}+HCO_3^-$ (c) Ca^{2+} *vs* SO_4^{2-} (d) TDS *vs* $Ca^{2+}+Mg^{2+}+HCO_3^-/Na^++K^++Cl^-+SO_4^{2-}$

3.4 Groundwater isotopes

The use of stable isotopes is key to determining groundwater sources and evolution [41]. Isotopic methodologies are well known nowadays in groundwater network hydrological studies [42]. Stable oxygen and hydrogen isotopes in groundwater give the original isotopic composition of rainwater recharging in the hydrological cycle [41-43]. They can include details on rainfall, evaporated surface water, and sources of seawater within the coordinate framework of ^{18}O which ^2H, and can therefore help to classify the causes of salinity in groundwater [44]. Table 3 indicates the $\delta^{18}O$ and δ^2H values of the groundwater samples tested. Stable isotopes of water points sampled in this study present a wide range of variation between –9.4 and –5.2 in $\delta^{18}O$ with a mean of –7.1 ± 1.3‰, and from –62.0 to –42.0 in δ^2H with a mean of –52.5 ± 5.6‰. In Figure 16, measured values of $\delta^{18}O$ and δ^2H from the investigated groundwater samples are compared with the global meteoric water line (GMWL: $\delta^2H = 8\ \delta^{18}O + 10$), defined by Craig [45]: the groundwater samples are distributed around a straight line intersecting the GMWL, with a slope equal to $\delta^2H = 2.2\ \delta^{18}O - 36.1$ (Figure 7). The aquifer's isotopic composition in δ^2H and $\delta^{18}O$ shows two classes of water that are virtually identical. The first category contains water samples strongly associated with the GMWL, demonstrating no major evaporation isotopic changes and that the aquifer regeneration is very fast. This group comprises primarily of wells (1, 15, 13, 6, 11, 19 and 22) located to the North of the recharge zone and two wells (7 and 14) located to the South of the plain secondarily. The second category is near below the meteoric water level, suggesting that the evaporation of groundwater [46, 47] and the salt waters of the lake have affected it. This group comprises basically of the wells located in the discharge region to the South of the plain (Figure 16).

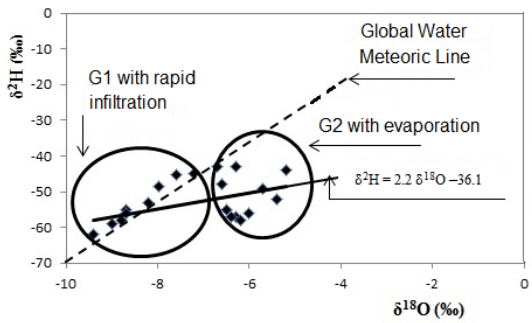

Figure 16. δ^2H versus $\delta^{18}O$ relationship for groundwater in the Hodna area

4. CONCLUSION

A groundwater quality evaluation of the Hodna region based on 25 groundwater samples shows that water class $Ca–HCO_3$ is present in the North of the study area, which characterizes low-mineralization waters, situated at higher elevations in recharge areas. Another essential form of water is the SO_4^{2-}-Cl^--Na^+ one, found primarily along the salt water lake in the South of the study region, characterizing high-mineralization waters. FA and CA multivariate statistical were used in this study for understanding the spatial and temporal patterns and controlling factors of groundwater geochemistry in the regional aquifer of the Hodna Plain, Algeria. The major conclusions related to understanding the regional scale groundwater geochemistry are as follows: the cluster analysis method can be applied for investigating both spatial and temporal patterns of groundwater geochemistry. This is done by first classifying monitoring data of groundwater geochemistry into clusters and then examining spatial and

temporal variations of the clusters to understand controlling factors of groundwater geochemistry based on hydrogeochemical analysis.

The first factor of FA was related to salinity parameters (EC, Na+, SO_4^{2-} and HCO_3^-), the second one to the carbonate content (Mg^{2+} and Ca^{2+}), the third one is mostly associated with evaporite host rocks (Cl^-) and chemical fertilizers content (K^+ and NO_3^-). Thus, FA provided a general understanding of the processes involved in groundwater chemical evolution. Samples were grouped into classes based on their similarities with CA. The G1 with low salinity (EC<1700µS/cm), G2 with high salinity (EC>2900µS/cm) and G3 with intermediate and average salinity (1700<EC< 2900µS/cm). It is just the G1 and G3 waters that can be used. On the other side, owing to the high salinity samples, the waters of G2 are not exploitable due to the flow inversion coming from the Hodna salt water lake to the middle of the plain, while this lake was initially the largest natural discharge region. The Multivariate statistics indicate that the three classified groups are statistically and geochemically reasonable.

The aquifer's isotopic composition in δ^2H and $\delta^{18}O$ shows two classes of water that are virtually identical. The first group demonstrates no major isotopic modifications through evaporation, which implies that the recharge of the aquifer at the northern boundary is very fast. The second party suggests that groundwater in the discharge region has been affected by evaporation and by the salt water of the Hodna Lake.

ACKNOWLEDGMENTS

The authors greatly appreciate the constructive and thoughtful comments of the anonymous reviewers they also thank the Editors-in-Chief of International Journal of Sustainable Development and Planning for his kind cooperation.

REFERENCES

[1] UNEP (United Nations Environmental Program) (1999). Global Environmental outlook 2000, Earthscan, UK. https://wedocs.unep.org.

[2] Benabderrahmane, A. (1988). Numerical simulations of salt pollution of an aquifer system in a semi-arid to arid - Sample aquifer systems of the plain of M'Sila- (Hodna, Algeria). PhD Thesis, UFR Applied Geology. Franche Comte. France. https://sudoc.fr.

[3] NAWR (National Agency for Water Resources) (1996). Survey of water wells and boreholes and of flows of the Chott El-Hodna (in French), Technical report, Ministry of Water Resources, Algeria.

[4] Amroune, A. (2008). Hydrogeology and groundwater quality of M'Sila area, Northwestern basin of the Hodna, Algeria). PhD thesis, University of Batna 2, Batna, Algeria. http://theses.univ-batna.dz.

[5] Nur, A., Ishaku, J.M., Tayib, A. (2012). Spatial distribution of chemical facies using geographical information system (GIS) in Michika, northeastern Nigeria. Research Journal in Engineering and Applied Sciences, 1(2): 102-109. http://scrip.org.

[6] Shahbazi, A, Esmaeili-Sari, A. (2009). Groundwater quality assessment in North of Iran: A case study of the Mazandaran province. World Applied Sciences Journal, 5(1): 92-97. http://citeseerx.ist.psu.edu.

[7] NAWR (National Agency for Water Resources) (2007). Modelling of the Hodna aquifer, Mission III model exploitation. Sub-Mission III 2 predictive simulation and proposal for optimum management of water resources (in French). Technical report. Icosium forage and engineering services. Ministry of Water Resources, Algiers, Algeria.

[8] Abdesselam, S., Merabet, Y., Halitim, A. (2007). Vulnerability of the functions of an agro-pastoral ecosystem to climate change (Case of Southern Hodna) (in French). International Days: The impact of climate change on arid and semi-arid region, CRSTRA, Biskra, Algeria. https://www.crstra.dz.

[9] Ophori, D.U., Tòth, J. (1989). Patterns of ground-water chemistry, Ross Creek Basin, Alberta, Canada. Ground Water, 27(1): 20-26. https://doi.org/10.1111/j.1745-6584.1989.tb00003.x

[10] Apodaca, L.E., Jeffrey, B.B., Michelle, C.S. (2002). Water quality in shallow alluvial aquifers, Upper Colorado River Basin, Colorado, 1997. Journal American Water Resources Association, 38(1): 133-143. https://doi.org/10.1111/j.1752-1688.2002.tb01541.x

[11] Drever, J.I. (1997). The Geochemistry of Natural Waters. Third eds., Journal of Environmental Quality, 27(1): 245-46. https://doi.org/10.2134/jeq1998.00472425002700010037x

[12] Kim, J.H., Kim, R.H., Lee, J.H., Cheong, T.J., Yum, B.W., Chang H.W. (2005). Multivariate statistical analysis to identify the major factors governing groundwater quality in the coastal area of Kimje, South Korea. Hydrology Process, 19(6): 1261-1276. https://doi.org/10.1002/hyp.5565

[13] Güler, C. Thyne, G.D. (2002). Geochemical evolution of surface and groundwater in Indian Wells-Owens valley area and surrounding ranges, southeastern California, USA. GSA Abstracts with Programs, 33, A16. https://www.researchgate.net/publication/309772846

[14] Mohapatra, P.K., Vijay, R., Pujari, P.R., Sundaray, S.K., Mohanty, B.P. (2011). Determination of processes affecting groundwater quality in the coastal aquifer beneath Puri City, India: A multivariate statistical approach. Water Science Technology, 64(4): 809-817. https://doi.org/10.2166/wst.2011.605

[15] Sebhi, S. (1987). Mutation of Rural World in Algeria-Case of Hodna (in French). Eds. OPU, Algiers. http://persee.fr.

[16] Abdesselam, S., Halitim, A., Jan A.F., Trolard, G., Bourrie, G. (2013). Anthropogenic contamination of groundwater with nitrate in arid region: Case study of southern Hodna (Algeria). Environmental Earth Sciences, 70: 2129-2141. https://doi.org/10.1007/s12665-012-1834-5

[17] Guiraud, R. (1973). Post-Triassic evolution of the country before the Alps according to the study of Hodna Basin and neighboring regions. PhD thesis, University of Nice, France. https://searchworks.stanford.edu.

[18] Standard methods for the Examination of Water and Wastewater (APHA) 2nd edn, American Public Health Association/American Water works Association/Water Environment Federation, Washington DC, USA, 2005. https://www.standardmethods.org.

[19] Winston, R.B. (2000). Graphical User Interface for

MODFLOW, Version 4. U.S. Geological Survey Open-File Report 00-315, 27p. https://doi.org/10.3133/ofr00315
[20] ESRI (2020). Topo to Raster. Online Tool References. https://pro.arcgis.com/en/pro-app/tool-reference/3d-analyst/topo-to-raster.htm.
[21] Dagnelie, P. (2006). Theoretical and applied statistics. Vol 2: Inferences one-and two-dimensional. Eds, Boeck and Larcier, Bruxelles. http://www.dagnelie.be/stpres.html.
[22] Laaksoharju, M., Gurban, I., Skarman, C., Skarman, E. (1999). Multivariate mixing and mass balance (M3) calculations, a new tool for decoding hydrogeochemical information. Applied Geochemistry, 14(7): 861-871. https://doi.org/10.1016/S0883-2927(99)00024-4
[23] Bartlett, M.S.A. (1954). Notes on multiplying factors for various chi-squared approximations. Journal of the Royal Statistical Society, Series B, 16: 296-298.
[24] Joshi, D.M., Bhandari, N.S., Kumar, A., Agrawal, N. (2009). Statistical analysis of physicochemical parameters of water of river Ganga in Haridwar district. Rasayan Journal of Chemistry, 2(3): 579-587.
[25] Kaiser, H.F. (1970). A second generation little jiffy. Psychometrika, 35: 401-415. https://doi.org/10.1007/BF02291817
[26] Amroune A., Boudoukha, A., Boumazbeur, A., Benaabidate, L., Guastaldi, E. (2017). Groundwater geochemistry and environmental isotopes of the Hodna area, Southeastern Algeria. Desalination and Water Treatment, 73: 225-236. https://doi.org/10.5004/dwt.2017.20642
[27] Kannan, N., Joseph, S. (2010). Quality of groundwater in the shallow aquifers of a paddy dominated agricultural river basin, Kerala, India. International Journal of Civil and Environmental Engineering, 3: 160-178.
[28] Hutchinson, M.F. (1988). Calculation of hydrologically sound digital elevation models. Paper presented at Third International Sympsium on Spatial Data Handling at Sydney, Australia.
[29] Hutchinson, M.F. (1989). A new procedure for gridding elevation and stream line data with automatic removal of spurious pits. Journal of Hydrology, 106(3-4): 211-232. https://doi.org/10.1016/0022-1694(89)90073-5
[30] Geller, W., Friese, K., Herzsprung, P., Kringel, R., Schultze, M. (2000). Limnology of sulphur-acidic mining lakes. II Chemical properties: The main constituents and buffering systems. Internationale Vereinigung für Theoretische und Angewandte Limnologie: Verhandlungen, 27(4): 2475–2479. https://doi.org/10.1080/03680770.1998.11901686
[31] OGRA (Official Gazette of the Republic of Algeria) (2013). n°18 of March 23, Executive Decree n°11–125 of March 22, 2011 relating to the quality of water for human consumption. http://www.cntppdz.com.
[32] Uzuakpunwa, A.B. (1981). The geochemistry and origin of the evaporite deposits in the southern half of the Benue Trough. Earth Evolution Sciences., 2: 136-138. http://pascal-francis.inist.fr.
[33] Vasant, G., Krishnamurthy, V.N., Sudha, G., Manik, D., Kalyani, P. (2009). The Fertilizer Encyclopedia. (eds) John Wiley & Sons, 8 avr. 872 p. https://www.wiley.com.
[34] Dalton, M.G., Upschurch S.B. (1978). Interpretation of hydrochemical facies by factor analysis. Groundwater, 16(4): 228-233. http://doi.org/10.1111/j.1745-6584.1978.tb03229.x
[35] Naseem, S., Hamza, S., Bashir, E. (2010). Groundwater geochemistry of winder agricultural farms, Balochistan, Pakistan and assessment for irrigation water quality. European Water, 31: 21-32.
[36] Yousef, A.F., Saleem, A.A., Baraka, A.M., Aglan, O.S.H. (2009). The impact of geological setting on the groundwater occurrences in some wadis in Shlatein-Abu Ramad Area, SE Desert, Egypt. European Water, 25(26): 53-68.
[37] Gibbs, R.J. (1970). Mechanisms controlling world's water chemistry. Science, 170(3962): 1088-1090. https://doi.org/10.1126/science.170.3962.1088
[38] Garrels, R.M., MacKenzie, F.T. (1967). Origin of the chemical compositions of some springs and lakes. In: Equilibrium Concepts in Natural Waters, American Cancer Society, Washington., DC. http://dx.doi.org/10.1021/ba-1967-0067.ch010
[39] Meybeck, M. (1987). Global chemical weathering from surficial rocks estimated from river dissolved loads. American Journal of Science, 287: 401-428. https://doi.org/10.2475/ajs.287.5.401
[40] Capaccioni, B., Didero, M., Paletta, C., Idero, L. (2005). Saline intrusion and refreshening in a multilayer coastal aquifer in the Catania Plain (Sicily, Southern Italy): dynamics of degradation processes according to hydrochemical characteristics of groundwaters. Journal of Hydrology, 307(1-4): 1-16. https://doi.org/10.1016/j.jhydrol.2004.08.037
[41] Fontes, J.Ch., Yousfi, M., Allison, G.B. (1986). Estimation of long term, diffuse groundwater discharge in the northern Sahara using stable isotope profiles in soil water. Journal of Hydrology, 86(3-4): 315-327. https://doi.org/10.1016/0022-1694(86)90170-8
[42] Gonfiantini, R., Conrad, G., Fontes, J.C., Sauzay, G., Payne, B.R. (1974). Etude isotopique de la nappe du continental intercalaire et de ses relations avec les autres nappes du Sahara septentrional. In: Proceedings of IAEA Symposium on Isotope Techniques in Groundwater Hydrology, Vienna, 227-241. https://inis.iaea.org.
[43] Fritz, P., Fontes, J.C. (1980). Handbook of Environmental Isotope Geochemistry. Elsevier, Amsterdam, p.2. https://inis.iaea.org.
[44] Gat, J., Carmi, L. (1970). Evolution of the isotopic composition of atmospheric waters in the Mediterranean Sea area. Journal of Geophysics Research, 75(15): 3039-3048. http://doi.org/10.1029/JC075i015p03039
[45] Craig, H. (1961). Isotopic variations in meteoric waters. Science, 133(3465): 1702-1703. http://doi.org/10.1126/science.133.3465.1702
[46] Edmunds, W.M., Guendouz, A.H., Mamou, A., Moulla, A., Shand, P., Zouari, K. (2003). Groundwater evolution in the continental intercalaire aquifer of southern Algeria and Tunisia: trace element and isotopic indicators. Applied Geochemistry, 18(6): 805-822. http://doi.org/10.1016/S0883-2927(02)00189-0
[47] Guendouz, A., Moulla, A.S., Edmunds, W.M., Zouari K., Shand, P., Mamou, A. (2003). Hydrogeochemical and isotopic evolution of water in the complex terminal aquifer in the Algerian Sahara. Hydrogeology Journal, 11(4): 483-495. http://doi.org/10.1007/s10040-003-0263-7